

Effect of temperature history and restraint degree on cracking behavior of early-age concrete

Jianda Xin^{a,b}, Guoxin Zhang^{a,b,*}, Yi Liu^{a,b}, Zhenhong Wang^{a,b}, Zhe Wu^{a,b}

^a State Key Laboratory of Simulation and Regulation of Water Cycle in River Basin, China Institute of Water Resources and Hydropower Research, A-1 Fuxing Road, Beijing 100038, PR China

^b Department of Structures and Materials, China Institute of Water Resources and Hydropower Research, A-1 Fuxing Road, Beijing 100038, PR China

HIGHLIGHTS

- A temperature stress testing machine was employed.
- Effect of temperature history and restraint degree was investigated.
- A high-low cooling rate history improved the cracking potential of concrete.
- The relationship between restraint degree and temperature difference was established.

ARTICLE INFO

Article history:

Received 23 February 2018

Received in revised form 8 October 2018

Accepted 9 October 2018

Keywords:

Early-age

Temperature history

Restraint degree

Cracking behavior

ABSTRACT

This study experimentally investigated the effect of temperature history and restraint degree on cracking behavior of early-age concrete, including cracking temperature, cracking stress/strength, creep/free deformation and cracking potential. The deformation, temperature and stress were measured with two different temperature histories and three different restraint degrees via a temperature stress testing machine (TSTM). The results show that, under different temperature histories, the magnitude of cracking potential of concrete was found to vary significantly. The concrete with a high-low cooling rate at early-age had better anti-cracking performance (improved by at least 13.1%) due to the more effective utilization of creep on reducing restrained stress. The high-low cooling rate history showed more outstanding effect on lowering cracking risk of concrete under higher restraint degree. Furthermore, an analytical method for establishing the relationship between the restraint degree and temperature difference was recommended for assessing cracking risk of concrete.

© 2018 Elsevier Ltd. All rights reserved.

1. Introduction

At early age, the temperature inside of massive structures during concrete hydration process can reach 40 °C [1–3]. Due to the time-dependent material behaviors of concrete (e.g. elastic modulus, creep, tensile strength and thermal deformation) and restraints caused by foundations and adjoining structures, the tensile stress of concrete is generated when the temperature of concrete gradually decreases. Cracks occur when the tensile stress of concrete exceeds its tensile strength [4–8].

Temperature control of massive concrete structures is one of the most effective methods to limit the magnitude of tensile stress.

The conventional recommendation is to keep the temperature drop (the difference between maximum temperature and ambient temperature) at a tolerant value [9–11]. For some cases, however, concrete still cracked when maximum temperature was deliberately controlled and the reason was attributed to the unreasonable cooling rate [12,13].

The effect of cooling rate on the cracking behavior of concrete has attracted attention from researchers and some restrained tests (e.g. ring and linear specimen test) have been conducted to evaluate the cracking behavior of early-age concrete regarding temperature variations, however, observations of tests seem different [14,15]. Briffaut et al. [14] investigated the effect of heating rate on the cracking behavior of concrete using ring specimens and found that the temperature difference (the difference between maximum temperature and cracking temperature) ΔT with higher rate was increased. Shi et al. [15] reported that ΔT increased with lower cooling rate using a temperature stress testing machine

* Corresponding author at: Department of Structures and Materials, China Institute of Water Resources and Hydropower Research, A-1 Fuxing Road, Beijing 100038, PR China

E-mail address: zhanggx@iwhr.com (G. Zhang).

(TSTM). These findings have demonstrated that the relationship between the cooling rate and the cracking behavior of concrete needs to be further explored.

Restraint degree is another crucial factor of evaluating restrained stress development and cracking potential. The restraint degree varies with the boundary condition and the geometry of structure. A comprehensive understanding of the restraint degree is vital for the sake of its significant effect on restrained stress, as well as cracking risks. Usually, the restraint degree of concrete structure decreases with the increasing distance from the contact surface between the concrete structure and the basement [10,16]. Several tests regarding 100% restraint degree have been conducted by researchers [17–19], however, few work has been designed to investigate the effect of varying restraint degrees. Though the restraint degree-related criterion is important, it has been mostly disregarded in the current concrete engineering. It is crucial to realize the complexity of restrained stress analyze in early-age massive concrete structures that a conventional constant restraint degree condition as such is too harsh, resulting in increment of construction costs and inaccurate optimizations of concrete mixture proportion. Thus, in addition to the ΔT -related cracking criterion [20,21], it is meaningful to establish a relationship between the restraint degree and the cracking behavior of concrete.

The aim of this paper is to investigate the effect of cooling rate and the restraint degree on cracking behavior of concrete. In practice, the cooling rate of massive concrete structures can approximately reach 0.5 °C/day [13,22]. Thus, two different temperature histories were selected to experimentally explore the effect of cooling rate on cracking behavior of concrete. Three restraint degrees with 100%, 75% and 50% were applied on restrained specimens via TSTM. Moreover, the coefficient of thermal expansion (CTE) and mechanical properties of concrete, such as splitting tensile strength and elastic modulus, were also studied to complement results of restrained test.

2. Experimental programs

2.1. Materials and mixture proportions

The concrete mixtures were made of ordinary Portland cement, fly ash, natural sand and gravel with a maximum particle size of 40 mm. Table 1 shows the mixture proportions of concrete.

2.2. Methods

2.2.1. Equipment

A TSTM which was firstly developed by Springenschmid et al. [23], then improved by others [24,25], was employed in the current research. Usually, this setup has two dog bone-shaped concrete specimens, one of which is unloaded and used for free deformation measurement, while the other is loaded under restrained condition. Dimensions of restrained specimens are identical to those of free specimens. A linear voltage displacement transducers (LVDT) is mounted on the straight part of specimens for recording the deformation. The temperature evolution of specimen can be controlled by the molds equipped with copper pipes of circulating ethylene glycol from a heating-cooling bath. One end of the restrained specimen is fixed and the other is connected to a servo motor (as shown in Fig. 1). The specimen is pulled/pushed to the original length once the deformation reaches a limit value [24,26]. Details of this kind of device can be found elsewhere [27,28].

In this study, the degree of restraint γ_R is defined as [16]:

$$\gamma_R = \frac{\varepsilon^{fr} - \varepsilon^{res}}{\varepsilon^{fr}} \quad (1)$$

Table 1
Mixture proportions of concrete (kg/m³).

Cement	Water	Fly ash	Sand	Gravel	Water reducer	Air-entraining admixture
108	83	58	539	1776	0.996	0.02656

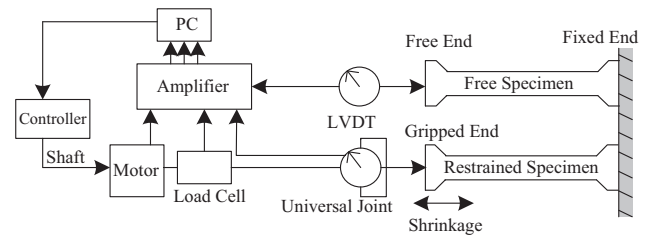


Fig. 1. Schematic description of the closed loop instrumented restraining system [24].

where ε^{fr} is the free deformation of concrete; ε^{res} is the residual deformation of restrained concrete.

Eq. (1) can also be rewritten as

$$\varepsilon^{res} = (1 - \gamma_R)\varepsilon^{fr} \quad (2)$$

When the restraint degree is chosen, ε^{res} of restrained specimen calculated by Eq. (2) then can be controlled by a servo motor.

2.2.2. Temperature history

For massive concrete structures, the temperature of concrete after casting gradually increases with hydration process of cement and the maximum temperature is deliberately designed and controlled for prevention of concrete cracking [13,29]. A field-measured temperature rise history (phase I) was employed to study the early-age behavior of concrete in the current research, as shown in Fig. 2. Since the cross section of massive concrete structures is very thick, the cooling rate of internal concrete is relatively slow (0.5–1 °C/day [13,22]) compared with that of thin-walled concrete structures (0.35 °C/h [14]). In order to investigate the effect of temperature history (i.e. the same temperature difference, but various cooling rates) on cracking behavior of concrete, two different temperature cooling rate histories, namely, a 1.0 °C/day–0.39 °C/h (high-low) and a 0.5 °C/day–0.6 °C/h (low-high) temperature history, were designed. As shown in Fig. 2, two different cooling rates were firstly selected in phase II; after 250 h, the cooling rates of specimens were then increased until concrete cracked and this period was denoted as phase III.

2.2.3. Calculation procedure of deformation

For fresh concrete, it is of great importance to determine the “starting point” of deformation measurement since the deformation strongly relates to the restrained stress. Meanwhile, the deformation before the “starting point” usually can be ignored since the stiffness of fresh concrete is relatively weak and no stress is generated. According to the literature [30], there is no consensus on the definition of “starting point”. In the current research, the “starting point” of deformation is defined as the time when the restrained stress started to develop [31,32], and can be easily monitored by a load cell.

The composition of residual deformation of concrete ε^{res} can be described by the following equation:

$$\varepsilon^{res}(t) = \varepsilon^e(t) + \varepsilon^{cr}(t) + \varepsilon^{fr}(t) \quad (3)$$

where $\varepsilon^e(t)$ is the elastic strain of concrete; $\varepsilon^{cr}(t)$ is the creep strain of concrete; $\varepsilon^{fr}(t)$ is the total free strain of concrete.

The elastic strain of concrete can be calculated by Eq. (4)

$$\varepsilon^e(t) = \frac{\sigma(t)}{E_c(t)} \quad (4)$$

where $E_c(t)$ is the elastic modulus of concrete at age of t .

The residual deformation of restrained concrete ε^{res} can be deduced by Eq. (2) based on a selected restraint degree, thus, the creep deformation of concrete $\varepsilon^{cr}(t)$ is the only unknown parameter and can be calculated by Eq. (3).

Fig. 3 shows the photo of TSTM and the dimensions of specimen are illustrated in Fig. 4.

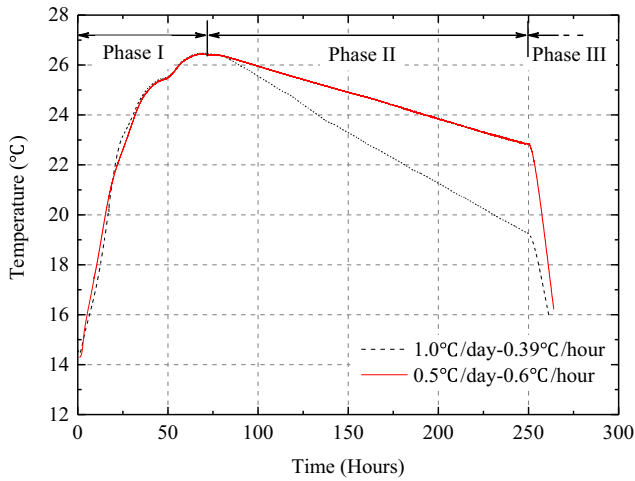


Fig. 2. Temperature histories of concrete specimens.

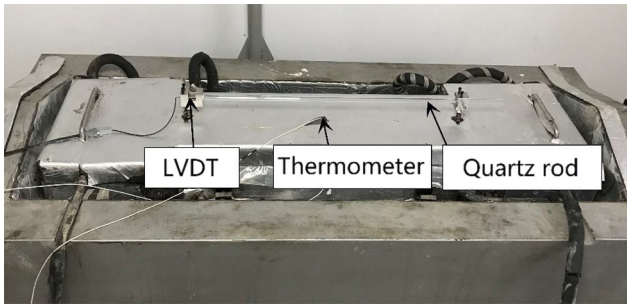


Fig. 3. Photo of TSTM.

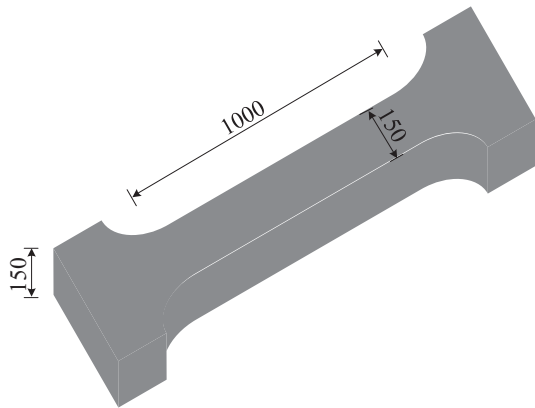


Fig. 4. Dimensions of the TSTM specimen (Unit: mm).

2.3. Mechanical properties, deformation and restrained stress measurement

2.3.1. Mechanical properties

According to the Chinese code GB/T 50081-2002 [33], the mechanical properties of concrete mixtures were measured on specimens of 100 mm × 100 mm × 300 mm for elastic modulus test and 100 mm × 100 mm × 100 mm for splitting tensile test.

2.3.2. Deformation measurement

Deformations of specimens under different temperature histories were measured through an LVDT mounted on the straight part of specimen, as shown in Fig. 3. The lateral and bottom sides of specimens were wrapped with plastic sheets

to minimum friction between the molds and specimens and the surface sides were wrapped with plastic sheets to prevent water loss. The specimens were designed to go through a three-phase temperature variation (Fig. 2): a temperature rise phase (approximately 65 h), a slow cooling temperature phase and a rapid cooling temperature phase. As mentioned above, the “start age” of measurement was identical to the time when the axial force started to develop in the restrained specimen.

2.3.3. Coefficient of thermal expansion (CTE)

It is reported that the CTE α became stable after 1 day [31,34]. The measurement of CTE was conducted on the free specimen 1 day after concrete casting under a designed temperature cycle via TSTM. For the sake of temperature stabilization in the cross section of specimen, temperature cycles ranging from 21 °C to 29 °C were performed for 100 h at the rate of 2 cycles per day [35]. Fig. 5(a) shows that the deformation and the temperature curves shared a similar trend and the calculated CTE was approximately 7.5 $\mu\epsilon/^\circ\text{C}$ (as shown in Fig. 5(b)).

2.3.4. Uniaxial restrained stress

The concrete mixture was directly cast into the molds of TSTM, then, all specimens were immediately sealed. The temperature histories of restrained specimens were identical to those of free specimens. The restraint and temperature history were applied on specimens immediately after casting, then data of temperature, deformation and stress of specimens were measured throughout the test. The cooling temperature phase lasted until the concrete cracked.

Three restraint degrees with 100%, 75% and 50% were adopted to study the relationship between cracking behavior and restraint degree. For each temperature history and restraint degree, two specimens were tested. It is found that the variation in the cracking temperature was less than 4%, which was satisfactory and confirmed the good reproducibility of the present research.

Parameters of tests are listed in Table 2. Each test is named following Eq. (5).

$$S \begin{matrix} - & XX & - & X \\ \text{restraint degree} & & \text{temperature history} & \end{matrix} \quad (5)$$

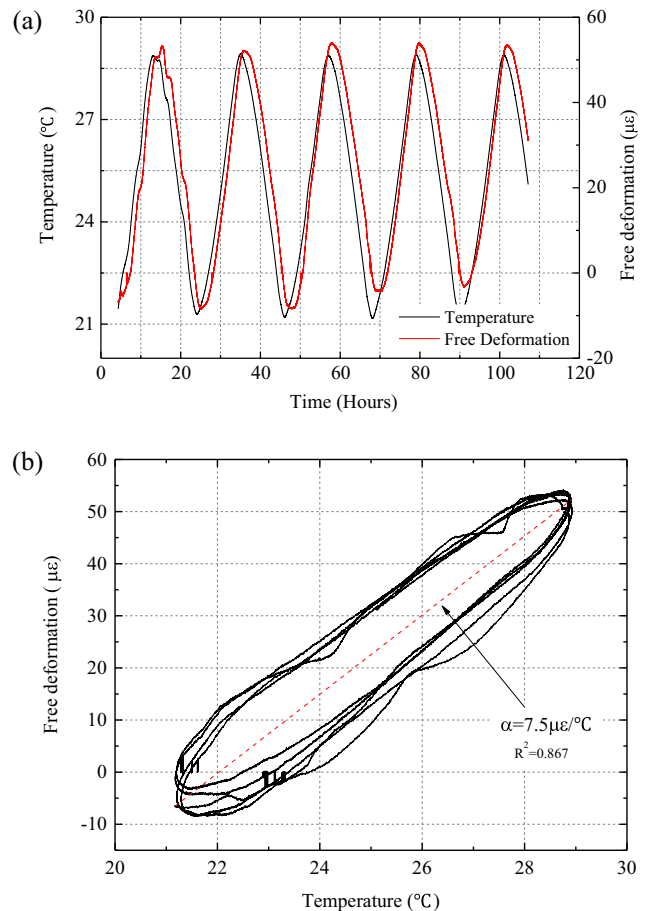


Fig. 5. CTE test results: (a) measured deformation and temperature; (b) calculated CTE.

Table 2
Parameters of tests.

Test	Temperature history	Restraint degree
S-100%-1 °C/day-0.39 °C/h	1 °C/day-0.39 °C/h	100%
S-75%-1 °C/day-0.39 °C/h	1 °C/day-0.39 °C/h	75%
S-50%-1 °C/day-0.39 °C/h	1 °C/day-0.39 °C/h	50%
S-100%-0.5 °C/day-0.6 °C/h	0.5 °C/day-0.6 °C/h	100%
S-75%-0.5 °C/day-0.6 °C/h	0.5 °C/day-0.6 °C/h	75%
S-50%-0.5 °C/day-0.6 °C/h	0.5 °C/day-0.6 °C/h	50%

3. Results and discussions

3.1. Evolution of mechanical properties

Fig. 6(a) and (b) show the evolutions of elastic modulus and splitting tensile strength of concrete mixtures under an isothermal curing condition, respectively.

The elastic modulus of concrete at age of 1 day, 3 days, 7 days and 28 days were 6.1 GPa, 20.1 GPa, 28.8 GPa and 36.8 GPa, respectively. The average increase rate during the first 3 days was almost 4 times of that from 3 days to 7 days. Besides, the elastic modulus of concrete at 7 days was up to 78.3% of that at 28 days.

The optimally approximated relationship between the elastic modulus and the age can be expressed as [13]

$$E(t) = E_{28}[1 - \exp(-at^b)] \quad (6)$$

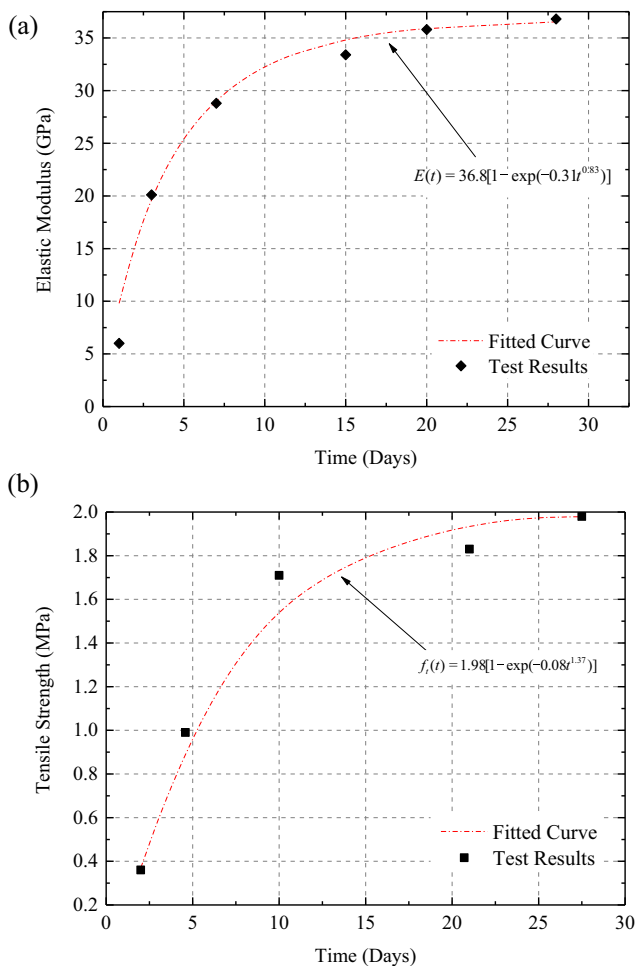


Fig. 6. Evolutions of concrete mechanical properties: (a) elastic modulus; (b) splitting tensile strength.

where E_{28} is the elastic modulus of concrete at 28 days, a and b are constants which can be determined from the experimental data.

The value of E_{28} , a and b were 36.8, 0.31 and 0.83, respectively. The obtained fit curve in Fig. 6(a) shows the fitness of the experimental data with the proposed equation (Eq. (6)).

The evolution of splitting tensile strength of concrete shared a similar trend with that of elastic modulus. The optimally approximated relationship between the splitting tensile strength and the age can be expressed by Eq. (7) [13]

$$f_{sp}(t) = f_{sp,28}[1 - \exp(-at^b)] \quad (7)$$

where $f_{sp,28}$ is the splitting tensile strength of concrete at 28 days.

As shown in Fig. 6(b), the value of $f_{sp,28}$, a and b were 1.98, 0.08 and 1.37, respectively.

The mechanical properties of concrete are strongly influenced by the temperature variation and an equivalent age concept [36] should be adopted to calculate related parameters. For an arbitrary temperature history $T(t)$, concrete age can be converted to equivalent age t_e via an Arrhenius law [37]

$$t_e = \int \exp\left[\frac{E_h}{R}\left(\frac{1}{T_0} - \frac{1}{T}\right)\right] dt \quad (8)$$

where E_h is the activation energy (J/mol); R is the ideal gas constant (J/mol/K); T_0 is the reference temperature and T is the actual temperature (K). E_h equals 33500 J/mol for the temperature $T \geq 20$ °C and 33500 + 1470(20 - T) J/mol for the temperature $T \leq 20$ °C [37]. T_0 equals 293.15 K.

It should be noted that the time t in the above equations should be converted into the corresponding equivalent age for subsequent strain analysis.

3.2. Evolution of restrained stress

Fig. 7(a) and (b) show the evolutions of temperature and restrained stress with two temperature histories, respectively. In phase I, due to the rapid hydration process of cement, temperature gradually raised and reached 26.4 °C at 65 h. Meanwhile, compressive stresses started to develop due to the restrained thermal deformation. As shown in Fig. 7(a), the maximum compressive stresses were -0.54 MPa, -0.41 MPa and -0.28 MPa for the restraint degree of 100%, 75% and 50%, respectively. It also can be seen from Fig. 7(a) that the ages of maximum compressive stress were earlier than those of maximum temperature, and this is due to the high relaxation property of early-age concrete [38,39]. In phase II, the temperature of specimens decreased at a specific cooling rate and the evolution of restrained stress was closely related to the relevant temperature. At a critical point, the compressive stress converted to tensile stress and this point is called the “second-zero-stress” age and the corresponding temperature is named as “second-zero-stress” temperature [16,40,41]. It is also observed from Fig. 7(a) that, the “second-zero-stress” temperature was higher than the initial temperature due to the increasing stiffness and high relaxation property of concrete at early-age [18,38,42]. After that, tensile stress increased and when it exceeded the tensile strength of concrete, cracks occurred.

Fig. 7(b) shows the evolutions of temperature and restrained stress with a cooling temperature history of 0.5 °C/day-0.6 °C/h. As expected, the stress evolution of concrete followed closely to the temperature history. It is shown that, the trends of compressive stress evolution (0–65 h) in Fig. 7(b) were almost the same compared with those in Fig. 7(a), however, followed by slower compressive stress decrease periods, leading to later “second-zero-stress” ages.

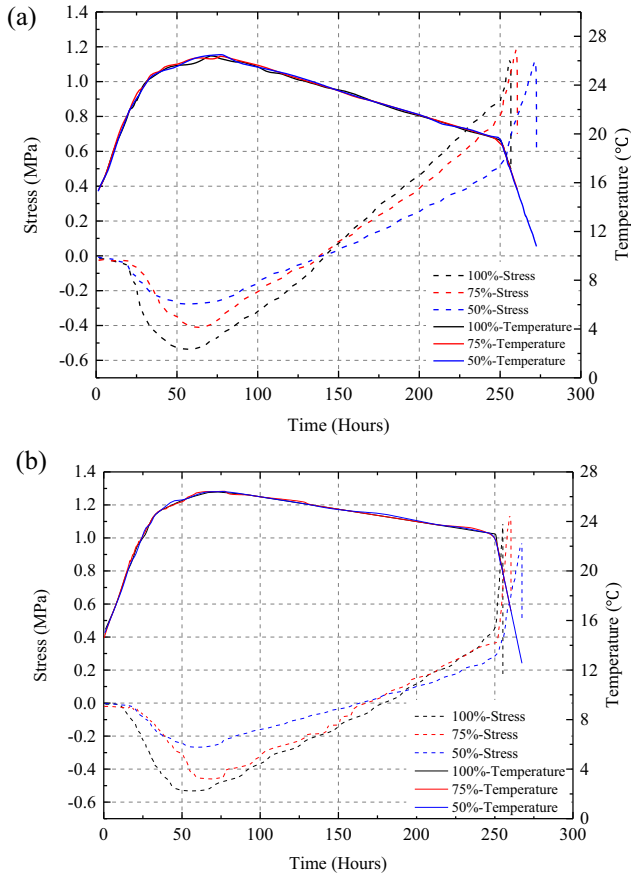


Fig. 7. Evolutions of concrete restrained stress with a cooling rate of (a) 1.0 °C/day-0.39 °C/h; and (b) 0.5 °C/day-0.6 °C/h.

3.3. Evolution of strain

Based on the strain calculation procedure mentioned in the section of 2.2, the free strains along with the elastic strains and creep strains under different temperature histories are depicted in Figs. 8 (a)–(c) and 9(a)–(c). For example, as shown in Fig. 8(a), the compressive creep strain gradually increased with the compressive stress and the rate decreased during the relaxation period. After the “second-zero-stress” age, the creep strain curve reversed, which means tensile creep strain started to develop and followed closely to the evolution of tensile stress [32,43].

3.4. Cracking behavior

3.4.1. Cracking stress

Stress evolutions of specimens with different temperature histories are shown in Fig. 7. The abrupt stress drop represents the cracking of concrete. The ratios of cracking stress to tensile strength of all specimens are denoted in Fig. 10. Generally, ratios of all specimens when cracked were less than 1.0 and nearly in the range of 0.6–0.8 [18,27]. The splitting tensile strength of concrete is usually measured via a rapid loading test, which differs from the slow loading process conducted by TSTM [44]. Furthermore, microcrackings are generated during frequent restraints applied by TSTM, leading to a relatively low cracking stress. Altoubat and Lange [45] found that this ratio was approximately 0.6–0.72 for normal concrete. Wei and Hansen [18] discovered that this ratio was approximately 0.8.

It also can be seen from Fig. 10 that the ratios of cracking stress to tensile strength under the low restraint degree were lower. This

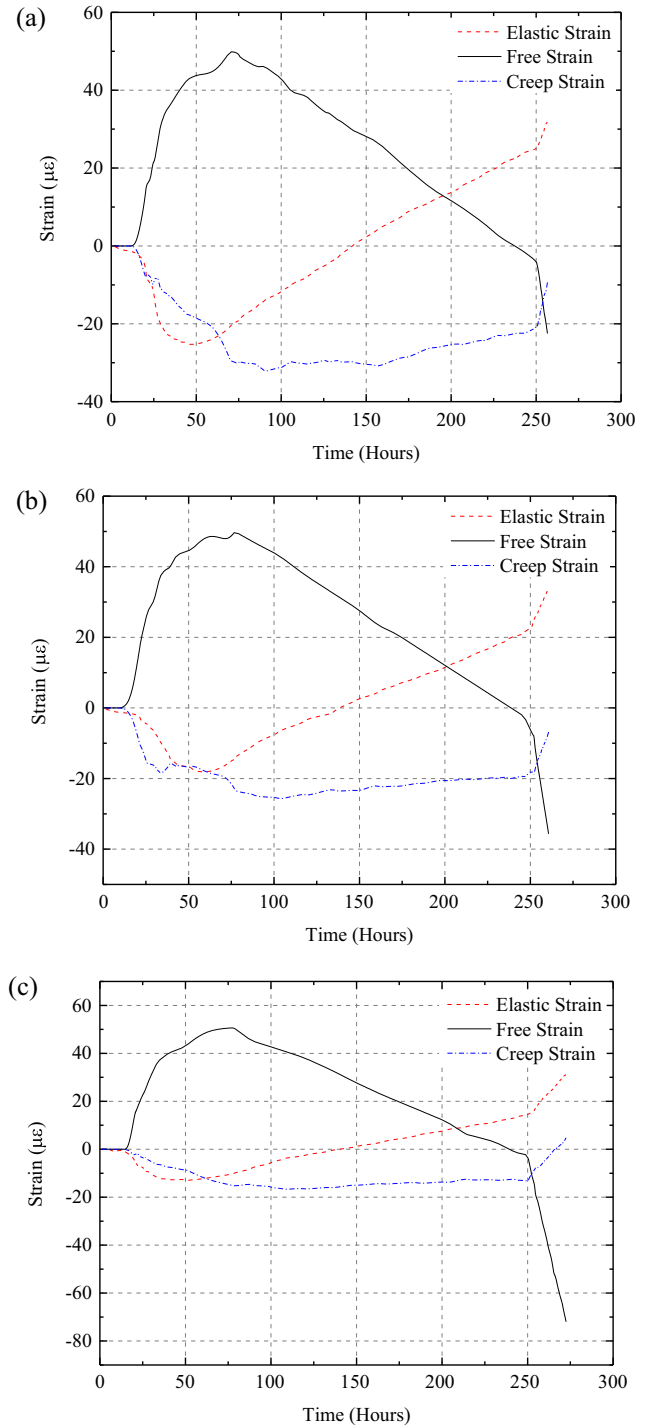


Fig. 8. Evolutions of concrete strains with a cooling rate of 1.0 °C/day-0.39 °C/h under the restraint degree of (a) 100%; (b) 75%; and (c) 50%.

reduction in strength can be related to fatigue and internal damage accumulation (microcrackings) under the slower sustained loading period [44,46,47].

3.4.2. Temperature difference ΔT

A series of parameters of temperature can be collected after concrete casting, such as casting temperature, maximum temperature, and cracking temperature, however, it is not precise enough to investigate the cracking behavior of concrete with these isolated

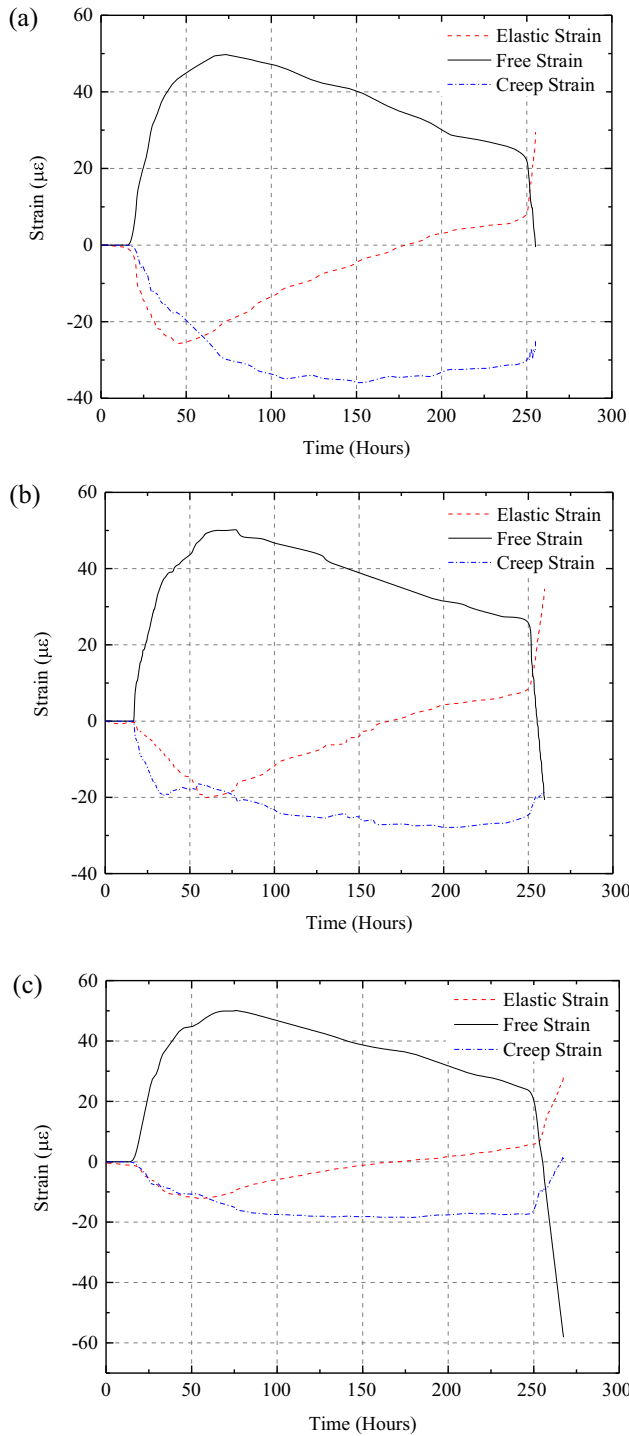


Fig. 9. Evolutions of concrete strains with a cooling rate of 0.5 °C/day-0.6 °C/h under the restraint degree of (a) 100%; (b) 75%; and (c) 50%.

parameters [40]. It is well known that the single temperature rise does not lead to concrete cracking but the temperature drop is more predominant on tensile stress evolution, as shown in Eq. (9) [14,40,48].

$$\sigma = \Delta T \alpha R \epsilon_R \tag{9}$$

where R is the relaxation modulus of concrete.

In this paper, the temperature difference ΔT is defined as

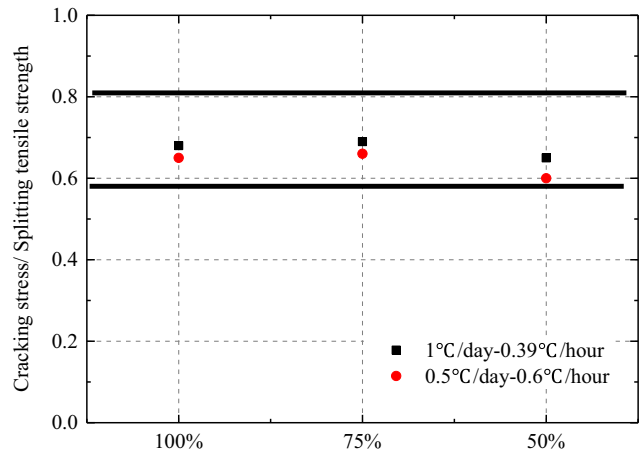


Fig. 10. Cracking stress/Splitting tensile strength of TSTM specimens.

$$\Delta T = T_{max} - T_{cr} \tag{10}$$

where T_{cr} is the temperature at concrete cracking age; T_{max} is the maximum temperature of concrete.

Fig. 11 shows the temperature differences of TSTM specimens. The temperature differences for the restraint degree of 100%, 75% and 50% with a cooling rate history of 1.0 °C/day-0.39 °C/h were 9.32 °C, 11.1 °C and 15.7 °C, respectively. As expected, the higher restraint degree leads to smaller temperature difference and the reason can be attributed to the higher tensile stress evolution caused by the higher restraint degree. Meanwhile, the temperature differences of specimens for the restraint degree of 100%, 75% and 50% with a cooling rate history of 0.5 °C/day-0.6 °C/h were 6.5 °C, 9.23 °C and 13.88 °C, respectively. It is interesting to note that under the same restraint degrees, the temperature differences of specimen with a cooling rate history of 1.0 °C/day-0.39 °C/h were higher than those with a cooling rate history of 0.5 °C/day-0.6 °C/h. The increase rates of temperature difference were 43.4%, 20.3% and 13.1% for the restraint degree of 100%, 75% and 50%, respectively. These results indicate that the effect of cooling rate on concrete cracking behavior is not constant but closely related to the concrete age and restraint degrees also have considerable effect on cracking behavior of concrete.

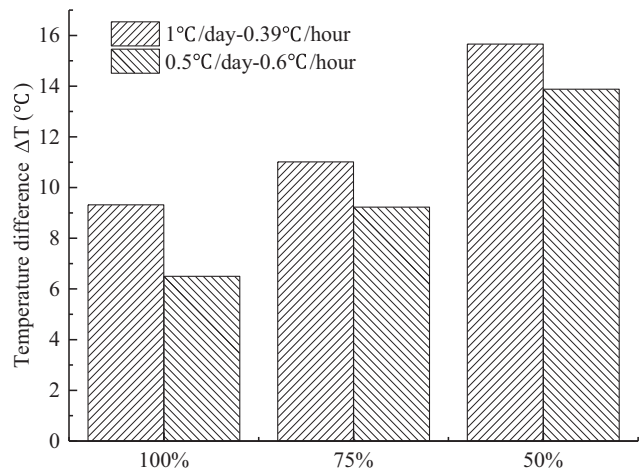


Fig. 11. Temperature differences of TSTM specimens.

3.5. Discussions

3.5.1. Effect of cooling rate on cracking behavior

Quantifying restrained stress and evaluating associated cracking behavior of concrete require many factors, such as creep/relaxation, temperature variation and deformation rate [4,49,50]. Several factors, such as specific creep and creep coefficient, have been employed to investigate creep behavior of concrete [4,51].

It is generally accepted that high creep property of early-age concrete is beneficial for lowering the cracking potential and more than 50% of restrained stress can be relaxed [47,52]. Creep, which is a time-dependent behavior, can be considered as a positive factor on reduction of cracking potential driven by free deformation, as shown in Eq. (11) [53]

$$p = \varepsilon^{fr} - (\varepsilon^e + \varepsilon^{cr}) \tag{11}$$

where p is the cracking potential of concrete.

In this paper, a creep-to-free strain ratio ψ is adopted to study the effect of cooling rate on cracking behavior of concrete [45,50] and can be expressed as

$$\psi = \frac{\varepsilon^{cr}}{\varepsilon^{fr}} \tag{12}$$

This ratio is a relevant index on evaluating the relationship between the creep and the free strain, as well as the relaxation property. It is proposed to calculate the creep-to-free deformation ratio from the age at which both the elastic strain and the change in creep strain become positive (i.e. “second-zero-stress” age) [31].

The creep strain and free strain can be obtained from section 3.3 and the creep-to-free deformation ratios of all specimens are shown in Fig. 12. It is shown that the creep-to-free deformation ratios of different restraint degrees shared a similar trend and the restraint degree of 100% condition showed the largest creep-to-free deformation ratio. This phenomenon can be interpreted to microcrackings (creep) under high stress/strength ratios [54–56].

It is worthwhile to compare the creep-to-free deformation ratios under different temperature histories to further investigate the effect of temperature histories on cracking behavior of concrete. It can be seen from Fig. 12(a) and (b) that the creep-to-free deformation ratios with the cooling rate history of 1.0 °C/day–0.39 °C/h were larger than those with the cooling rate history of 0.5 °C/day–0.6 °C/h, indicating that creep behavior on reduction of restrained stress was more predominant. This phenomenon can be explained by the fact that by more efficiently using stronger creep property of concrete at early-age, more restrained stress (i.e. temperature drop) can be relaxed and the cracking potential accordingly was lowered. Furthermore, the effect of temperature history on cracking behavior of concrete also can be obtained by analyzing restrained stresses under the same temperature drop. It is observed from Fig. 8 (a) and (b) that the restrained stress of concrete under the restraint degree of 100% with a cooling rate history of 1.0 °C/day –0.39 °C/h was 0.77 MPa at a temperature of 20 °C, which was smaller than that with a cooling rate history of 0.5 °C/day –0.6 °C/h (1.06 MPa), which have proven the positive effect of early age cooling on reduction of restrained stress. This result also agrees well with the obtained temperature differences under different temperature histories (as shown in Fig. 11).

There have been several indexes on assessment of cracking potential of concrete, such as restrained stress/strength [49,57], elastic strain/strain capacity [58], cracking age [59], and cracking temperature [60,61], etc. According to ASTM standard [62], two criteria, namely the net time of cracking in the ring test (time from the initiation of drying) and the stress rate, were recommended. A modified criterion Φ combining these two criteria, which was proposed by Kovler and Bentur [63], also has been used to investigate

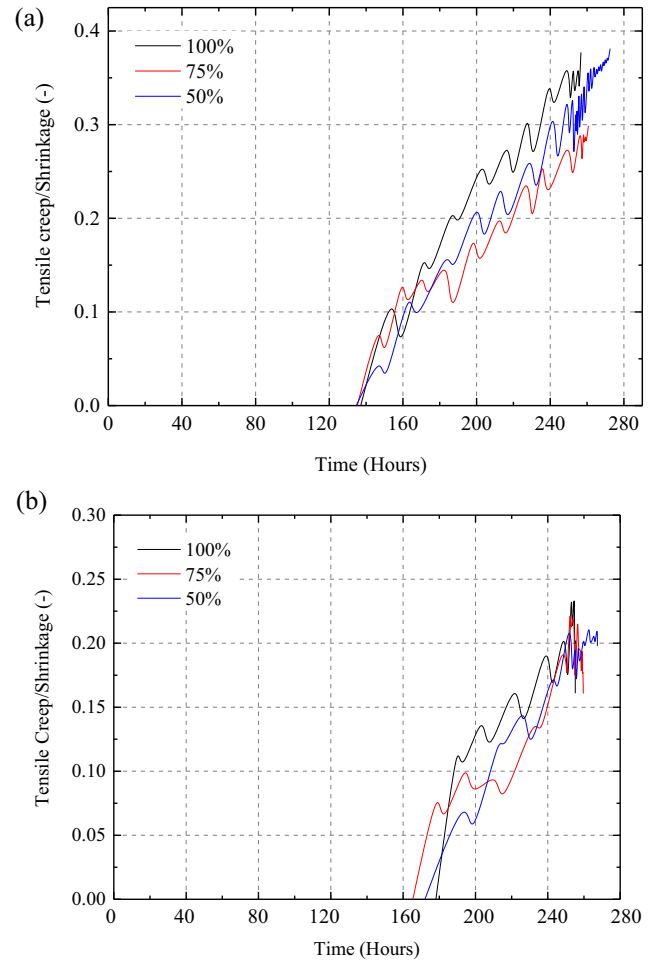


Fig. 12. Tensile creep/Shrinkage of TSTM specimens under the cooling rate of (a) 1.0 °C/day-0.39 °C/h; and (b) 0.5 °C/day-0.6 °C/h.

the cracking potential of concrete under different restraint conditions, as shown in Eq. (13).

$$\Phi = \frac{S}{t_{cr}} \tag{13}$$

where S is the stress rate, and t_{cr} is the net time of cracking.

A similar integrated criterion, which was recommended by Shen et al. [61], is adopted in this paper to investigate cracking potential of concrete in the TSTM test, as shown in Eq. (14)

$$\Phi = \frac{S}{t_{cr}} \tag{14}$$

where t_{cr} is the net time of cracking (time from the initiation of tensile stress).

As shown in Eq. (14), the higher integrated criterion value represents that concrete is more prone to cracking. The calculated results of cracking potential are shown in Fig. 13. It can be concluded that the integrated criterion values with the cooling rate history of 1.0 °C/day-0.39 °C/h were globally lower than those with the cooling rate history of 0.5 °C/day-0.6 °C/h under the same restraint degrees, indicating that concrete mixture with a high-low cooling rate history had lower cracking potential (i.e. larger temperature difference).

3.5.2. Effect of restraint degree on cracking behavior

As shown in Eq. (9), the restrained stress depends not only on the free deformation of concrete, but also on the restraint degree.

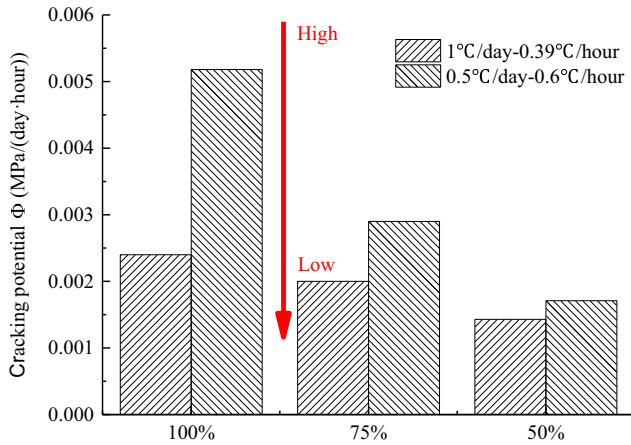


Fig. 13. Cracking potentials of TSTM specimens.

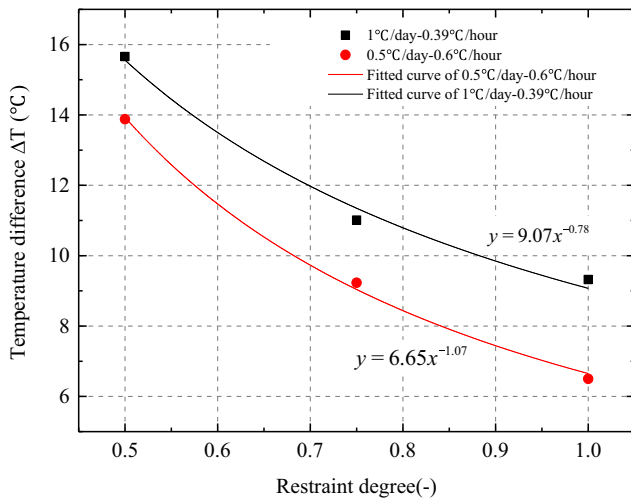


Fig. 14. The relationships between the temperature difference and the restraint degree.

This factor also should be studied to evaluate cracking behavior of concrete.

As mentioned in Section 3.4, the temperature differences of concrete with the cooling rate history of 1.0 °C/day-0.39 °C/h were generally larger due to the effective use of creep behavior of early age concrete. It is also interesting to note that with the higher restraint degree, the effect of high-low cooling rate on improvement of temperature difference became more predominant. For example, based on the obtained temperature difference from TSTM tests, the increase rate of allowable temperature differences under the restraint degree of 100% at early-age was 2 times larger than that under the restraint degree of 50% (as shown in Fig. 11). This

phenomenon is related to the tussle between the evolution of restrained stress and strength. The strength of concrete at early age was rapidly increasing (as shown in Fig. 6), while the positive effect of high-low cooling rate can effectively lower the magnitude of tensile stress, and the coupling effect of lowering restrained stress and increasing tensile strength therefore postponed the cracking age of concrete to some extent.

The relationships between the restraint degree and the temperature difference have been depicted in Fig. 14. The optimally approximated relationship between the restraint degree and the temperature difference can be expressed by Eq. (15).

$$y = ax^b \tag{15}$$

where a and b are constants and can be obtained from the experimental data.

The values of a under the cooling rate history of 1.0 °C/day-0.39 °C/h and 0.5 °C/day-0.6 °C/h are 9.07 and 6.65, respectively. The values of b under the cooling rate history of 1.0 °C/day-0.39 °C/h and 0.5 °C/day -0.6 °C/h are -0.78 and -1.07, respectively. It should be note that Eq. (15) is an empirical formulation, however, this relationship helps engineers to approximately estimate the cracking potential of massive concrete structures without making complex calculation.

3.5.3. An analytical method for calculation of temperature difference

In this section, a simple analytical method is introduced for analysis of temperature differences under different restraint degrees and temperature histories.

Based on Eqs. (1) and (11), one can obtain the relationship between ε^{fr} , ε^e and ε^c when concrete cracks

$$\gamma_R \varepsilon^{fr} = \varepsilon^e + \varepsilon^c \tag{16}$$

Substituting Eq. (12) into Eq. (16) and assuming $\varepsilon^{fr} = \alpha \Delta T_1$, the temperature difference ΔT_1 can be expressed as

$$\Delta T_1 = \frac{\varepsilon^e}{\alpha \gamma_R (1 - \psi)} \tag{17}$$

where ΔT_1 is the temperature difference between age of “second-zero-stress” and cracking.

Then, the temperature difference ΔT can be obtained by Eq. (18)

$$\Delta T = \Delta T_1 + \Delta T_2 \tag{18}$$

where ΔT_2 is the temperature difference between age of “second-zero-stress” and maximum temperature, which can be obtained from TSTM tests.

ε^e can be obtained from Figs. 8 and 9, and Ψ can be obtained from Fig. 12, then, the analytical temperature differences ΔT can be calculated. Table 3 shows the comparison of analytical and experimental values of temperature differences ΔT . Except for the case of S-50%-0.5 °C/day-0.6 °C/h, a good global accordance is obtained. The ΔT gap for the case of S-50%-0.5 °C/day-0.6 °C/h might be attributed to the variation of material parameters (e.g. α) caused by inhomogeneity of concrete, leading to inaccurate calculation results using Eq. (17).

Table 3 Comparison of ΔT of experimental and analytical value.

Temperature history	1.0 °C/day-0.39 °C/h			0.5 °C/day-0.6 °C/h		
Restraint degree (-)	1.0	0.75	0.5	1.0	0.75	0.5
$\alpha(\mu\varepsilon/^\circ\text{C})$	7.5					
$\varepsilon^e(\mu\varepsilon)$	32	33.5	31.1	29.5	34.7	29.1
$\psi(-)$	0.37	0.3	0.38	0.16	0.16	0.20
Experimental $\Delta T_2(^\circ\text{C})$	2.66	2.73	2.3	2.1	1.93	1.73
Analytical $\Delta T(^\circ\text{C})$	9.43	11.2	15.69	6.78	9.27	11.43
Experimental $\Delta T(^\circ\text{C})$	9.32	11.1	15.7	6.5	9.23	13.88

4. Conclusions

An experimental program was carried out to investigate the effect of temperature history and restraint degree on cracking behavior of early-age concrete. Two temperature histories and three restraint degrees were adopted to assess its effect on the restrained stress using TSTM. The following conclusions can be drawn from this study:

1. The cracking behavior of concrete closely relates to the temperature history, besides the temperature-related criterion. With a high-low cooling rate history at early age, a larger allowable temperature difference of concrete (improved by at least 13.1%) can be obtained in the current research.
2. The creep-to-free deformation ratio of concrete with the high-low cooling rate at early-age (0.3–0.38) was larger compared with that of concrete with the low-high cooling rate (0.16–0.2), resulting in higher efficient utilization of creep, as well as lower cracking potential of concrete. This phenomenon also confirms the vital role of creep behavior on stress relaxation of concrete.
3. The combination of temperature history and restraint degree led to various effects on cracking behavior of concrete: the high-low cooling rate history showed more outstanding effect on lowering cracking risk of concrete under higher restraint degree. In the current research, the increase rate of allowable temperature differences with the restraint degree of 100% was 2 times larger than that with the restraint degree of 50%.
4. A simple analytical method was introduced to establish the relationship between the restraint degree and the temperature difference, which can be utilized for cracking potential assessment under different realistic conditions.

Conflict of interest

Authors declare that they have no conflict of interest.

Acknowledgements

The authors would like to acknowledge the support provided by the National Key R&D Program of China (Grant No. 2016YFB0201000), the National Natural Science Foundation of China (Grant Nos. 51579252, 51439005, 51779277), the Special Scientific Fund sponsored by IWHR for Department of Structures and Materials, china (Grant Nos. SS0145B712017, SS0145B392016) and the Special Scientific Research Project of the State Key Laboratory of Simulation and Regulation of Water Cycle in River Basin of IWHR, china (Grant No. SS0112B102016). Support provided by China Three Gorges Corporation research project, china (Grant No. WDD/0428) is also gratefully acknowledged.

References

- [1] M. Azenha, R. Faria, Temperatures and stresses due to cement hydration on the R/C foundation of a wind tower—A case study, *Eng. Struct.* 30 (9) (2008) 2392–2400.
- [2] I. Yoshitake, H. Wong, T. Ishida, A.Y. Nassif, Thermal stress of high volume fly-ash (HVFA) concrete made with limestone aggregate, *Constr. Build. Mater.* 71 (2014) 216–225.
- [3] N. Bouzoubaa, M. Lachemi, Self-compacting concrete incorporating high volumes of class F fly ash: preliminary results, *Cem. Concr. Res.* 31 (3) (2001) 413–420.
- [4] I. Khan, A. Castel, R.I. Gilbert, Effects of fly ash on early-age properties and cracking of concrete, *ACI Mater. J.* 114 (4) (2017) 673–681.
- [5] H.K. Lee, K.M. Lee, B.G. Kim, Autogenous shrinkage of high-performance concrete containing fly ash, *Mag. Concr. Res.* 55 (6) (2003) 507–515.
- [6] S. Altoubat, M.T. Junaid, M. Leblouba, D. Badran, Effectiveness of fly ash on the restrained shrinkage cracking resistance of self-compacting concrete, *Cem. Concr. Compos.* 79 (2017) 9–20.
- [7] I. Pane, W. Hansen, Early age creep and stress relaxation of concrete containing blended cements, *Mater. Struct.* 35 (2) (2002) 92–96.
- [8] S. Altoubat, D. Badran, M.T. Junaid, M. Leblouba, Restrained shrinkage behavior of self-compacting concrete containing ground-granulated blast-furnace slag, *Constr. Build. Mater.* 129 (2016) 98–105.
- [9] China Standard SL191-2008, Design Code for Hydraulic Concrete Structures, 2015, Beijing.
- [10] ACI Committee 207, Effect of Restraint, Volume Change, and Reinforcement on Cracking of Mass Concrete (207.2R-95), Farmington Hills, Mich, 1995.
- [11] JSCE, Standard Specification for Concrete Structures-2007 Dam Construction, 2007, Tokyo.
- [12] H. Mihashi, F.H. Wittmann, Control of Cracking in Early Age Concrete, A. A. Balkema, Lisse, 2002.
- [13] B.F. Zhu, Thermal Stresses and Temperature Control of Mass Concrete, Butterworth-Heinemann, Oxford, 2013.
- [14] M. Briffaut, F. Benboudjema, J.M. Torrenti, G. Nahas, A thermal active restrained shrinkage ring test to study the early age concrete behaviour of massive structures, *Cem. Concr. Res.* 41 (1) (2011) 56–63.
- [15] N.N. Shi, J.S. Ouyang, R.X. Zhang, D.H. Huang, Experimental study on early-age crack of mass concrete under the controlled temperature history, *Adv. Mater. Sci. Eng.* 2014 (2014) 1–10.
- [16] T. Zhang, W.Z. Qin, Tensile creep due to restraining stresses in high-strength concrete at early ages, *Cem. Concr. Res.* 36 (3) (2006) 584–591.
- [17] D. Shen, J. Jiang, Y. Jiao, J. Shen, G. Jiang, Early-age tensile creep and cracking potential of concrete internally cured with pre-wetted lightweight aggregate, *Constr. Build. Mater.* 135 (2017) 420–429.
- [18] Y. Wei, W. Hansen, Early-age strain–stress relationship and cracking behavior of slag cement mixtures subject to constant uniaxial restraint, *Constr. Build. Mater.* 49 (2013) 635–642.
- [19] A.E. Klausen, T. Kanstad, Ø. Bjøntegaard, E. Sellevold, Comparison of tensile and compressive creep of fly ash concretes in the hardening phase, *Cem. Concr. Res.* 95 (2017) 188–194.
- [20] M. Eberhardt, S.J. Lokhorst, K.V. Breugel, On the reliability of temperature differentials as a criterion for the risk of early-age thermal cracking, in: R. Springenschmid (Ed.), *Thermal Cracking in Concrete at Early Age*, E & FN Spon, London, RILEM, 1994, pp. 353–360.
- [21] P.E. Roelfstra, T.A.M. Salet, J.E. Kuiks, Defining and application of stress analysis based temperature difference limits to prevent early-age cracking in concrete structures, in: R. Springenschmid (Ed.), *Thermal Cracking in Concrete at Early Age*, E & FN Spon, London, RILEM, 1994, pp. 273–280.
- [22] Z. Wang, Y. Liu, G. Zhang, W. Hou, Schematic study on temperature control and crack prevention during spillway tunnel concreting period, *Mater. Struct.* 48 (11) (2015) 3517–3525.
- [23] R. Springenschmid, R. Breitenbucher, M. Mangold, Development of the cracking frame and the temperature-stress testing machine, in: R. Springenschmid (Ed.), *Thermal Cracking in Concrete at Early Ages*, E & FN Spon, London, 1994, pp. 137–144.
- [24] K. Kovler, Testing system for determining the mechanical behavior of early age concrete under restrained and free uniaxial shrinkage, *Mater. Struct.* 27 (6) (1994) 324–330.
- [25] Z.H. Lin, W.Z. Qin, S.H. Zhang, T. Zhang, The application of virtual instrument technology in experimental evaluation of cracking sensitivity of concrete at early ages, *Ind. Constr.* 33 (7) (2003) 37–40 (in Chinese).
- [26] A. Darquennes, S. Staquet, M.P. Delplancke-Ogletree, B. Espion, Effect of autogenous deformation on the cracking risk of slag cement concretes, *Cem. Concr. Compos.* 33 (3) (2011) 368–379.
- [27] J.D. Xin, S.Q. Lin, N.N. Shi, D.H. Huang, Effect of reinforcement on early-age concrete temperature stress: preliminary experimental investigation and analytical simulation, *Adv. Mater. Sci. Eng.* 2015 (3) (2015) 1–9.
- [28] A. Darquennes, S. Staquet, B. Espion, Behaviour of slag cement concrete under restraint conditions, *Eur. J. Environ. Civ. Eng.* 15 (5) (2011) 787–798.
- [29] Y. Hu, G. Liang, Q. Li, Z. Zuo, A monitoring-mining-modeling system and its application to the temperature status of the Xiluodu arch dam, *Adv. Struct. Eng.* 20 (2) (2017) 235–244.
- [30] J. Weiss, Experimental determination of the time-zero (maturity-zero), in: A. Bentur (Ed.), *Early Age Cracking in Cementitious Systems*, Report of RILEM Committee TC 181-EAS, RILEM Publications Sarl, Bagneux, France, 2002, pp. 195–206.
- [31] D. Cusson, T. Hoogveen, An experimental approach for the analysis of early-age behaviour of high-performance concrete structures under restrained shrinkage, *Cem. Concr. Res.* 37 (2) (2007) 200–209.
- [32] D. Atrushii, Ø. Bjøntegaard, D. Bosnjak, T. Kanstad, E.J. Sellevold, Creep deformations in hardening concrete: test method investigations and the effect of temperature, in: L. Elfgrén (Ed.), *Report of Improved Production of Advanced Concrete Structures – IPACS (No 2001 BE96-3843)*, Luleå University of Technology, Luleå, Sweden, 2001, pp. 1–17.
- [33] China Standard GB/T50081-2002, Test Standards and Methods for Mechanical Properties of Normal Concrete, 2002, Beijing.
- [34] M. Viviani, B. Glisic, I.F.C. Smith, Separation of thermal and autogenous deformation at varying temperatures using optical fiber sensors, *Cem. Concr. Compos.* 29 (6) (2007) 435–447.

- [35] R. Springenschmid, R. Breitenbücher, Practical experience with concrete technology measures to avoid cracking, in: RILEM Int. Symposium on Avoidance of Thermal Cracking in Concrete, Munich, 1994.
- [36] E. Rastrup, Heat of hydration in concrete, *Mag. Concr. Res.* 6 (17) (1954) 79–92.
- [37] P. Hansen, E. Pedersen, Maturity computer for controlled curing and hardening of concrete, *Nord. Betong.* 1 (1977) 19–34.
- [38] L. Østergaard, D.A. Lange, S.A. Altoubat, H. Stang, Tensile basic creep of early-age concrete under constant load, *Cem. Concr. Res.* 31 (12) (2001) 1895–1899.
- [39] I. Khan, A. Castel, R.I. Gilbert, Tensile creep and early-age concrete cracking due to restrained shrinkage, *Constr. Build. Mater.* 149 (2017) 705–715.
- [40] R. Breitenbücher, Investigation of thermal cracking with the cracking-frame, *Mater. Struct.* 23 (3) (1990) 172–177.
- [41] J.H. Yeon, S. Choi, M.C. Won, Evaluation of zero-stress temperature prediction model for Portland cement concrete pavements, *Constr. Build. Mater.* 40 (2013) 492–500.
- [42] M.N. Amin, J.S. Kim, Y. Lee, J.K. Kim, Simulation of the thermal stress in mass concrete using a thermal stress measuring device, *Cem. Concr. Res.* 39 (3) (2009) 154–164.
- [43] D. Cusson, T. Hoogeven, Internal curing of high-performance concrete with pre-soaked fine lightweight aggregate for prevention of autogenous shrinkage cracking, *Cem. Concr. Res.* 38 (6) (2008) 757–765.
- [44] S.I. Igarashi, A. Bentur, K. Kovler, Autogenous shrinkage and induced restraining stresses in high-strength concretes, *Cem. Concr. Res.* 30 (2000) 1701–1707.
- [45] S.A. Altoubat, D.A. Lange, Tensile basic creep: measurements and behavior at early age, *ACI Mater. J.* 98 (5) (2001) 386–393.
- [46] S.A. Kaplan, Factors affecting the relationship between rate of loading and measured compressive strength of concrete, *Mag. Concr. Res.* 32 (111) (2015) 79–88.
- [47] S.A. Altoubat, D.A. Lange, Creep, shrinkage, and cracking of restrained concrete at early age, *ACI Mater. J.* 98 (4) (2001) 323–331.
- [48] A. Williams, A. Markandeya, Y. Stetsko, K. Riding, A. Zayed, Cracking potential and temperature sensitivity of metakaolin concrete, *Constr. Build. Mater.* 120 (2016) 172–180.
- [49] A.B. Hossain, J. Weiss, Assessing residual stress development and stress relaxation in restrained concrete ring specimens, *Cem. Concr. Compos.* 26 (5) (2004) 531–540.
- [50] H.T. See, E.K. Attiogbe, M.A. Miltenberger, Shrinkage cracking characteristics of concrete using ring specimens, *ACI Mater. J.* 100 (3) (2003) 239–245.
- [51] K. Kuder, D. Lehman, J. Berman, G. Hannesson, R. Shogren, Mechanical properties of self consolidating concrete blended with high volumes of fly ash and slag, *Constr. Build. Mater.* 34 (2012) 285–295.
- [52] H. Beushausen, C. Masuku, P. Moyo, Relaxation characteristics of cement mortar subjected to tensile strain, *Mater. Struct.* 45 (8) (2012) 1181–1188.
- [53] V.C. Li, High performance fiber reinforced cementitious composites as durable material for concrete structure repair, *Int. J. Restor. Build. Monum.* 10 (2) (2004) 163–180.
- [54] P. Rossi, J.L. Tailhan, F. Le Maou, L. Gaillet, E. Martin, Basic creep behavior of concretes investigation of the physical mechanisms by using acoustic emission, *Cem. Concr. Res.* 42 (1) (2012) 61–73.
- [55] A. Bentur, Early, Age Shrinkage Induced Stresses and Cracking in Cementitious Systems RILEM technical committee 191-EAS, RILEM Publications, 2003.
- [56] M.A. Al-Kubaisy, A.G. Young, Failure of concrete under sustained tension, *Mag. Concr. Res.* 27 (1975) 171–178.
- [57] A. Passuello, G. Moriconi, S.P. Shah, Cracking behavior of concrete with shrinkage reducing admixtures and PVA fibers, *Cem. Concr. Compos.* 31 (10) (2009) 699–704.
- [58] S.B. Keskin, M. Sahmaran, I.O. Yaman, M. Lachemi, Correlation between the viscoelastic properties and cracking potential of engineered cementitious composites, *Constr. Build. Mater.* 71 (2014) 375–383.
- [59] S. Tongaroon Sri, S. Tangtermsirikul, Effect of mineral admixtures and curing periods on shrinkage and cracking age under restrained condition, *Constr. Build. Mater.* 23 (2) (2009) 1050–1056.
- [60] K. Raoufi, J. Schlitter, D.P. Bentz, W.J. Weiss, Parametric assessment of stress development and cracking in internally cured restrained mortars experiencing autogenous deformations and thermal loading, *Adv. Civ. Eng.* (2011) 1–16.
- [61] D.J. Shen, J.L. Jiang, J.X. Shen, P.P. Yao, G.Q. Jiang, Influence of prewetted lightweight aggregates on the behavior and cracking potential of internally cured concrete at an early age, *Constr. Build. Mater.* 99 (2015) 260–271.
- [62] ASTM, Standard, test method for determining age at cracking and induced tensile stress characteristics of mortar and concrete under restrained shrinkage, Standard C 1581–04, ASTM Int, West Conshohocken (PA), 2013.
- [63] K. Kovler, A. Bentur, Cracking sensitivity of normal-and high-strength concretes, *ACI Mater. J.* 106 (6) (2009) 537–542.